IEEE Photonics Journal
An IEEE Photonics Society Publication

Open Access

Experimental Demonstration of Bidirectional OFDM/OQAM-MIMO Signal Over a Multicore Fiber System

Volume 8, Number 5, October 2016

Jiale He
Borui Li
Lei Deng
Ming Tang, *Senior Member, IEEE*
Lin Gan
Songnian Fu
Perry Ping Shum
Deming Liu

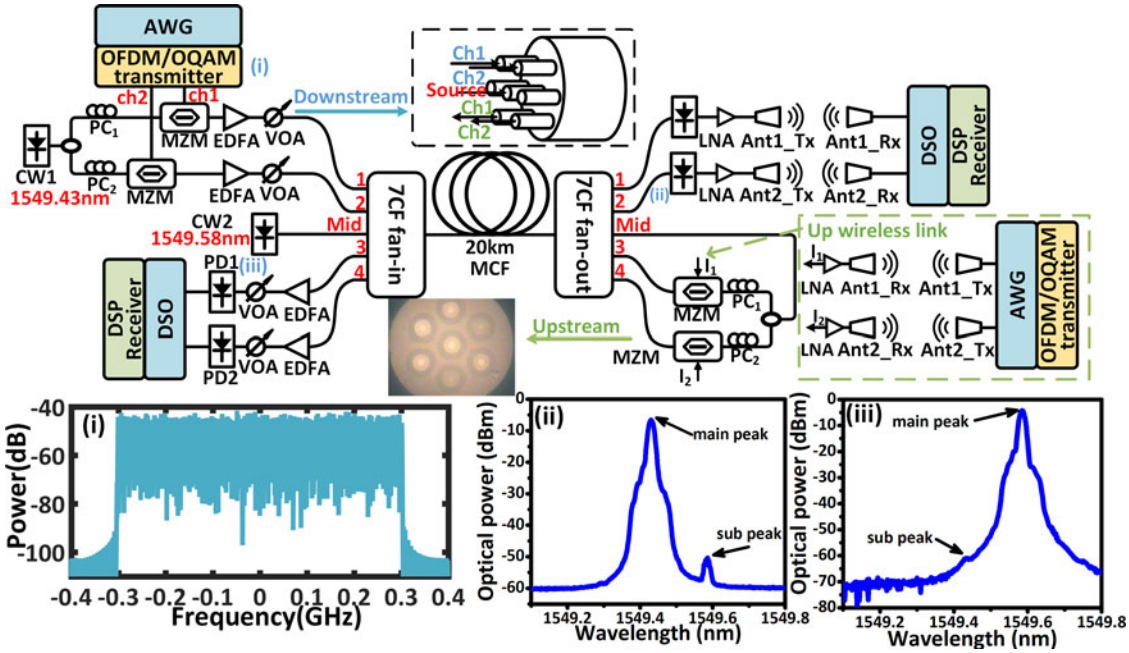

DOI: 10.1109/JPHOT.2016.2607203

IEEE photonics SOCIETY

IEEE

Experimental Demonstration of Bidirectional OFDM/OQAM-MIMO Signal Over a Multicore Fiber System

Jiale He,[1] Borui Li,[1] Lei Deng,[1] Ming Tang,[1] *Senior Member, IEEE*, Lin Gan,[1] Songnian Fu,[1] Perry Ping Shum,[2] and Deming Liu[1]

[1]Next Generation Internet Access National Engineering Laboratory, School of Optical and Electronic Information, Huazhong University of Science and Technology, Wuhan 430074, China.
[2]School of Electrical and Electronic Engineering, Nanyang Technological University, Singapore 639798, Singapore.

DOI:10.1109/JPHOT.2016.2607203

Manuscript received July 30, 2016; revised September 1, 2016; accepted September 5, 2016. Date of publication September 8, 2016; date of current version September 26, 2016. This work was supported in part by the National "863" Program of China under Grant 2015AA016904 and in part by the the National Nature Science Foundation of China under Grant 61675083, Grant 61307091, Grant 61275069, and Grant 61331010. Corresponding author: L. Deng (e-mail: denglei_hust@mail.hust.edu.cn).

Abstract: A bidirectional transmission and massive multi-input multi-output (MIMO) enabled radio over a multicore fiber system with centralized optical carrier delivery is experimentally investigated in this paper. Optical carriers for upstream are delivered from the central office to the remote antenna unit via the inner core for the coreless implementation. In our experiment, as one of the fifth-generation (5G) waveform candidates, orthogonal frequency division multiplexing using offset quadrature amplitude modulation (OFDM/OQAM) is adopted in both uplink and downlink to increase the spectral efficiency and side lobes suppression ratio. An advanced 2×2 MIMO-OFDM/OQAM channel estimation algorithm is optimally designed to equalize the hybrid optical and wireless MIMO channels. The experimental results show that bidirectional transmission of 4.46 Gb/s 2×2 MIMO-OFDM/16-OQAM could be achieved over a 20-km seven-core fiber and a 0.4-m wireless link. The proposed scheme proves that the multicore fiber can realize the transparent transmission of bidirectional radio signals and effectively simplify the infrastructures in the future 5G cellular systems.

Index Terms: Orthogonal frequency division multiplexing using offset quadrature amplitude modulation (OFDM/OQAM), multicore fiber (MCF), radio over fiber (RoF), optical communication

1. Introduction

Recently, fifth-generation (5G) mobile communication network technologies have been proposed to meet the explosive demand of mobile data capacity. It has been predicted that the 5G cellular system should be able to support 1000-fold gains in capacity and a 10 Gb/s individual user peak access rate experience [1]. To reach such high data rate, high-spectral-efficiency modulation format and massive multi-input multi-output (MIMO) technologies are indispensable. Moreover, radio over fiber (RoF) is also regarded as the considerable technique as it supports long-distance transmission and broadband wireless signals with centralized signal processing and low-cost implementation [2]. As one of the most popular modulation techniques, orthogonal frequency division multiplex (OFDM) has been

widely used in Long-Term Evolution (LTE) systems [3], [4]. The requirement of cyclic prefix (CP) will limit the spectral efficiency, although it is utilized to resist inter symbol interference (ISI) and inter carrier interference (ICI). To achieve better spectral efficiency (SE), as one of the filter bank multicarrier modulation format (FBMC), OFDM using offset quadrature amplitude modulation (OFDM/OQAM) is introduced [5], [6]. In OFDM/OQAM, the used filters with good localization in time and frequency domains not only sharp a higher side lobes suppression ratio of pulse spectrum but also help to resist ISI and ICI without using CP, leading to the increase of SE [5]. The high side lobe suppression ratio makes OFDM/OQAM more promising in narrow guard interval (GI) or carrier aggregation applications [6].

MIMO-based spatial multiplexing is another powerful technique for increasing channel capacity [7]. To deliver the signal to lots of antennas in the remote antenna units (RAUs), optical multiplexing techniques are required for low-cost implementation. Polarization division multiplexing (PDM) [8] and wavelength division multiplexing (WDM) [9] techniques are already considered in RoF systems. Moreover, optical space division multiplexing (SDM) technique based on multicore-fiber (MCF) has great potential for application in current LTE-advanced system [10], [11] and the future 5G cellular system, due to its compactness and spatial parallelism to support a lot of MIMO channels [12]. In general, the PDM technique can only provide two channels. The WDM technique is expensive due to the use of multi-wavelength laser sources. Actually, the MCF has the weakness of high cost in fiber and fan in/out devices fabrication, but the MCF also has the advantage of low inter-core crosstalk and supporting high spatial dimensions. We believe that MCF-based SDM technique has potential use in future cellular system for its high capacity of supporting massive MIMO implementation.

Recently, we have reported an experimental study on the transmission of three groups of 2×2 MIMO-OFDM/OQAM signals over 7-core MCF and wireless link and the impact of optical inter-core crosstalk in 7-core fibers on this radio over multi-core fiber [12]. However, the MCF-based RoF schemes mentioned above only focus on downlink transmission for demonstration purpose. Although a concept of reconfigurable radio access networks using multicore fiber has already been proposed in [13], no experimental verification has been done. Nevertheless, a more comprehensive investigation on the bidirectional RoF transmission based on multicore fiber is highly desired.

To further improve the transmission capacity and make MCF more feasible to deploy in practical 5G cellular system, in this paper, we propose a bidirectional $N \times N$ MIMO signal over $2N + 1$ core fiber system. Five spatial dimensions are used to experimentally demonstrate the bidirectional 2×2 MIMO OFDM/OQAM radio over 20 km 7-core MCF and 0.4 m wireless link. A total of 5 cores are used in this system, where the middle core is used to deliver the seed light to RAU for coreless upstream transmission, and four rest outer cores are used for bidirectional transmission. An advanced 2×2 MIMO-OFDM/OQAM channel estimation algorithm is optimally designed to equalize the hybrid optical and wireless MIMO channels. The experimental results show that the multicore fiber can transparently transmit radio MIMO channels with simplest wireless front haul configuration. Besides, the multicore fiber can also support large scale of MIMO channels with optimal design of high dense core fibers.

2. Principle

Fig. 1 illustrates the bidirectional $N \times N$ MIMO signal over $2N + 1$ core fiber system. For the downstream transmission, at the central office (CO) N channel input signals with the same RF frequency f_{RF} are modulated by an array of laser diode (LD). The generated optical signals are launched into N cores by the $2N + 1$ core fiber fan-in device, and then be captured by an array of photodiode (PD) after M-km MCF propagation and $2N + 1$ core fiber fan-out device. Subsequently, the N channel RF signals are fed into antenna array for wireless transmission. For the upstream transmission, a continuous wave (CW) laser with wavelength λ_{up} at the CO is delivered to RAU by using the middle core, and then be divided into N equal parts by a power splitter (PS). Each one is modulated by the received RF signal from antenna array at the optical modulator array. The generated N channel upstream signals are launched into the rest N cores and are then captured and recovered by an array of PD, the analog to digital convertor (ADC), and the digital signal process (DSP) module after M-km MCF propagation. The wavelength reuse technique is used in this structure where the

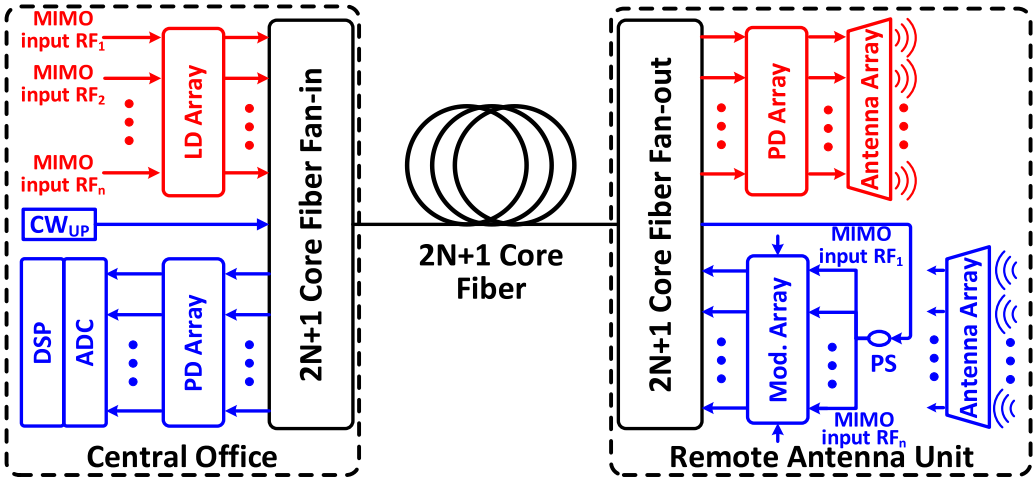

Fig. 1. Schematic of the bidirectional N × N MIMO radio over 2N + 1 core fiber system.

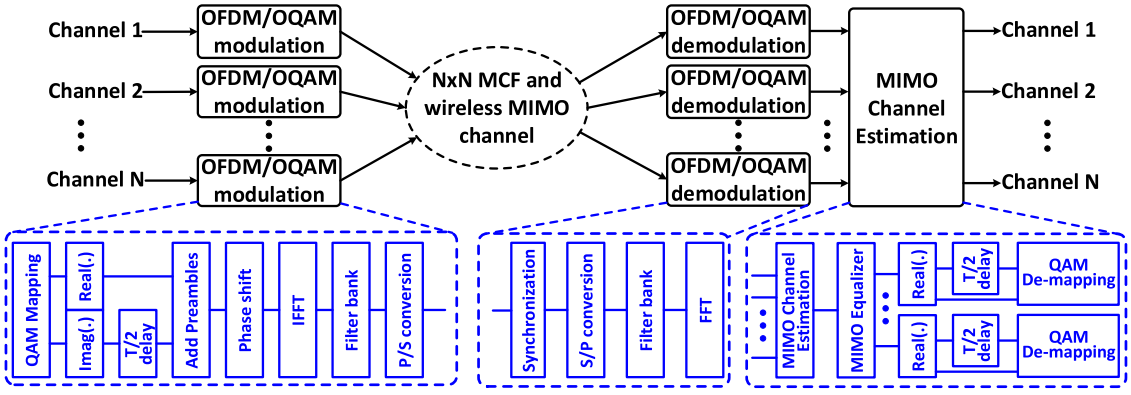

Fig. 2. Principle of DFT-based N × N MIMO-OFDM/OQAM system.

seed CW laser is delivered to RAU In RAU, the low-cost reflective semiconductor amplifiers (RSOA) array can be used to transmit the upstream data. Meanwhile, it should be noted that the seed light and upstream data are transmitted in different cores; thus, the Rayleigh backscattering effect from the seed light can be avoid.

Fig. 2 shows the operating principle of DFT-based N × N MIMO-OFDM/OQAM system [14]. N channel data streams are modulated by N OFDM/OQAM modulators respectively before MCF and wireless transmission. In each OFDM/OQAM modulator, the input data stream is mapped into QAM format. The real and imaginary part of the generated signal are separated and the imaginary part is delayed by half symbol period. Thus, the half symbol duration τ_0 and subcarrier spacing F_0 satisfy the condition $\tau_0 F_0 = 1/2$. After inserting preambles for channel estimation and synchronization, the phase of each point is shifted by $(m + n - 2) \times \pi/2$, where m is the index of subcarrier and n is the index of symbol. After IFFT, each symbol is filtered by a bank of FIR shaping filters. At last, a P/S converter is used to generate the baseband continuous-time OFDM/OQAM signal, which can be expressed as

$$S(t) = \sum_{m=0}^{M-1} \sum_{n=0}^{2N-1} a_{m,n} g(t - n\tau_0) e^{j2\pi m F_0 t} e^{j\frac{\pi}{2}(m+n-2)} \quad (1)$$

where $a_{m,n}$ is real valued offset-QAM data, $g(t)$ is the designed FIR filter, and τ_0 and $e^{j\pi(m+n-2)/2}$ are the additional phase terms for $a_{m,n}$.

After MCF and wireless transmission, N channel received signals are demodulated by N OFDM/OQAM demodulators, respectively, and then, the MIMO channel estimation module could be used to recover N channel data streams. In each OFDM/OQAM demodulator, synchronization, serial to parallel (S/P) conversion, FIR filters and FFT modules are used to transform the received signal into frequency domain. After hybrid channel estimation and MIMO equalization algorithm, the real field orthogonality in each channel could be maintained and then the obtained offset QAM signals could be transformed into QAM signals just by delaying half symbol period and combing back to the complex form again.

For the proposed bidirectional N $\times$ N MIMO RoF system, when considering the channel noises from both optical link and wireless link and taking 2 $\times$ 2 channels for example, the downlink MIMO channel model in frequency domain could be expressed as

$$\begin{aligned}\begin{bmatrix} y_1 \\ y_2 \end{bmatrix} &= \begin{bmatrix} h_{11} & h_{12} \\ h_{21} & h_{22} \end{bmatrix} \left(\begin{bmatrix} H_{Fcore1} & H_{Fcore2to1} \\ H_{Fcore2to1} & H_{Fcore2} \end{bmatrix} \begin{bmatrix} x_1 \\ x_2 \end{bmatrix} + \begin{bmatrix} n_1 \\ n_2 \end{bmatrix} \right) + \begin{bmatrix} w_1 \\ w_2 \end{bmatrix} \\ &\approx \begin{bmatrix} h_{11} & h_{12} \\ h_{21} & h_{22} \end{bmatrix} \begin{bmatrix} x_1 \\ x_2 \end{bmatrix} + \begin{bmatrix} h_{11}n_1 + h_{12}n_2 + w_1 \\ h_{21}n_1 + h_{22}n_2 + w_2 \end{bmatrix} \end{aligned} \tag{2}$$

where the matrix H_F represents the MCF channel of two cores. Because the inter-core crosstalk of the used MCF is below -45 dB/100 km, the interference terms in H_F could be neglected [15], [16]. n_1 and n_2 are the random noises in these two optical links. The matrix of h represents the wireless MIMO channel response, and w_1 and w_2 are the noises in wireless link.

Similarly, the uplink 2 $\times$ 2 MIMO channel model in frequency domain could be described as

$$\begin{aligned}\begin{bmatrix} y_1 \\ y_2 \end{bmatrix} &= \begin{bmatrix} H_{Fcore1} & H_{Fcore2to1} \\ H_{Fcore2to1} & H_{Fcore2} \end{bmatrix} \left(\begin{bmatrix} h_{11} & h_{12} \\ h_{21} & h_{22} \end{bmatrix} \begin{bmatrix} x_1 \\ x_2 \end{bmatrix} + \begin{bmatrix} w_1 \\ w_2 \end{bmatrix} \right) + \begin{bmatrix} n_1 \\ n_2 \end{bmatrix} \\ &\approx \begin{bmatrix} h_{11} & h_{12} \\ h_{21} & h_{22} \end{bmatrix} \begin{bmatrix} x_1 \\ x_2 \end{bmatrix} + \begin{bmatrix} n_1 + w_1 \\ n_2 + w_2 \end{bmatrix} \end{aligned} \tag{3}$$

where the matrix H_F and the matrix of h are the MCF and wireless link MIMO channel response, respectively, and the vector of $n_{1,2}$ and $w_{1,2}$ are the random noises from optical link and wireless channel respectively. Similarly, the interference items in H_F can be also ignored due to the lower inter-core crosstalk of the used MCF. Comparatively analyzing (2) and (3), it could be clearly observed that different noise distribution in optical and wireless links will lead to different transmission performance of uplink and downlink.

To simplify the analysis, we combine the MCF and wireless link into a hybrid channel and ignore the noises differences. The frequency domain channel model for both uplink and downlink could be expressed as

$$\begin{bmatrix} y_1 \\ y_2 \end{bmatrix} = \begin{bmatrix} hb_{11} & hb_{12} \\ hb_{21} & hb_{22} \end{bmatrix} \begin{bmatrix} x_1 \\ x_2 \end{bmatrix} + \begin{bmatrix} N_1 \\ N_2 \end{bmatrix}, \tag{4}$$

where $x_{1,2}$ and $y_{1,2}$ are the transmitted and the received signals for two channels, respectively, and $N_{1,2}$ are the unified hybrid channel noises. To estimate the hybrid MIMO channel response hb, the full loaded preambles of $[p,\ p]^T$ and $[p,\ -p]^T$ is used in our experiment [17]. By using the least square (LS) channel estimator and interference cancellation (IC) method [18], the estimated channel response can be easily calculated as

$$\begin{bmatrix} H_{11} & H_{12} \\ H_{21} & H_{22} \end{bmatrix} \approx \begin{bmatrix} y_{11} & y_{12} \\ y_{21} & y_{22} \end{bmatrix} \begin{bmatrix} p + jI_{p11} & p + jI_{p12} \\ p + jI_{p21} & -p + jI_{p22} \end{bmatrix}^{-1}, \tag{5}$$

where y_{11} and y_{12} stand for the received training symbols in one channel, like y_{21} and y_{22} for another channel. Matrix p and matrix H are the transmitted training symbols and estimated MIMO channel

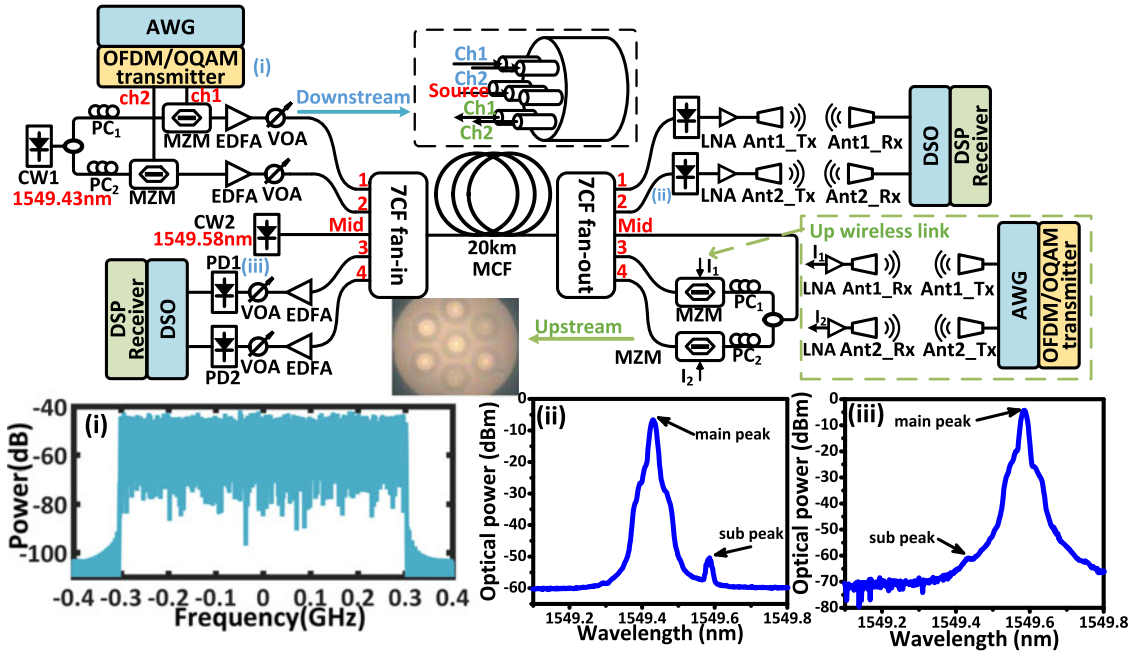

Fig. 3. Experimental setup of the proposed bidirectional N dimensional MIMO radio over 2N + 1 core fiber.

response, respectively, and symbol *I* represents the interference calculation. Finally, we can obtain the received signals by using the estimated channel response *H*.

3. Experimental Setup and Results

The experimental setup of the proposed scheme is shown in Fig. 3. At the central office (CO), an arbitrary waveform generator (AWG, AWG7122B) with a sample rate of 10 GSa/s is used to generate two-channel RF MIMO OFDM/OQAM signals. For each channel, 192 subcarriers of 16 offset QAM and 256-point IFFT are adopted for OFDM/OQAM modulation, and noting that no CP is used here. The used pulse shaping filter is raised root cosine with roll off factor of 1, and the filter length is four times the length of one symbol. We employ eight training symbols for every 100 payload symbols, where one is for time synchronization and two are for 2×2 MIMO channel estimation. The two MIMO training symbols are full loaded in a manner of $[A, A]^T$ and $[A, -A]^T$. These two generated baseband OFDM/OQAM signal are then up-converted to 2.2 GHz in the AWG. As a result, the net rate can reach to 4.42 Gb/s ($2 \times 10GSa/s/12.5 \times 4 \times (100-8)/100 \times 192/256$) with 600 MHz bandwidth ($10GSa/s/12.5 \times 192/256$). A 100 kHz-linewidth continuous-wave (CW) external cavity laser (ECL, $\lambda_1 = 1549.43$ nm) is used as the optical source for downstream. This optical source is firstly split into two parts by an optical coupler (OC). The two OFDM/OQAM signals are then modulated onto these two optical carriers by two Mach-Zehnder modulators (MZMs), respectively. Subsequently, these two optical signals are coupled into seven-core MCF by the self-developed fan-in/fan-out devices [19], [20] with low loss and low crosstalk. The used seven-core MCF have a step refractive index profile and low crosstalk of -45 dB/100 km between adjacent cores is achieved. The cross section view of this MCF is shown in the inset of Fig. 3. After 20 km MCF propagation and the fan-out device, the optical signals are detected by two 10 GHz bandwidth photodiodes (PD). After two lower noise amplifiers (LNAs) with 27 dB gain, the generated RF OFDM/OQAM signals are fed into two antennas. The horizontal spacing between two Tx antennas and two Rx antennas are both 0.1 m, and the vertical spacing between Tx antennas and Rx antennas are both 0.4 m. After 0.4 m air transmission, these two wireless signals are received by two receiver antennas and then

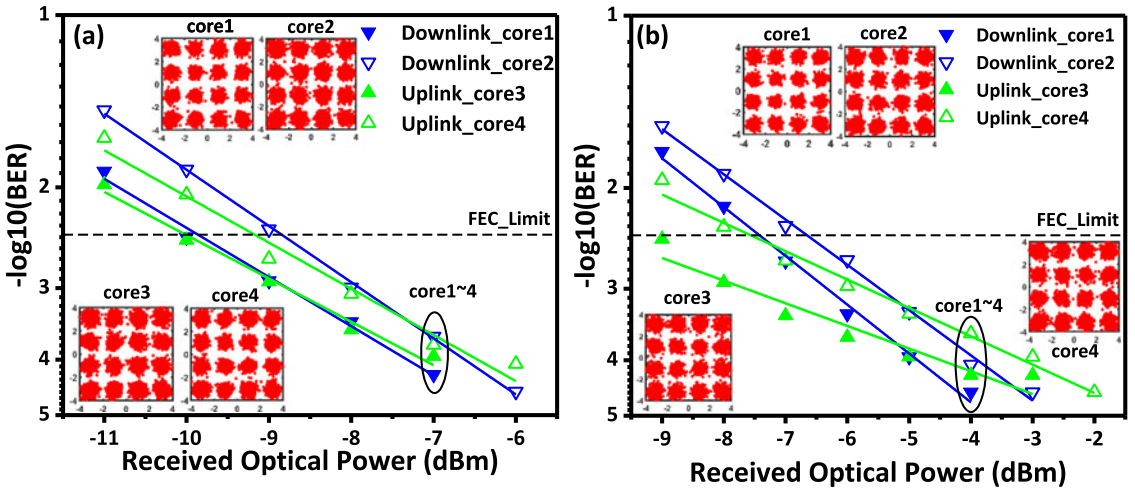

Fig. 4. BER performance of downlink and uplink in (a) without wireless link and (b) with wireless link.

captured by a 25 GSa/s digital sampling oscilloscope (DSO, Tektronix DPO72504DX). Offline signal processing including resampling, time synchronization, MIMO channel estimation, data mapping and BER counting is performed. A total of 7×10^5 bits are calculated for BER counting in our experiment. Inset (i) of Fig. 3 shows the electronic spectrum of the baseband OFDM/OQAM signal.

For the uplink transmission, another 100 kHz-linewidth continuous-wave (CW) external cavity laser (ECL, $\lambda_2 = 1549.586$ nm) is launched into the middle core of the MCF in CO. after 20 km MCF propagation, the seed source is split into two parts by an OC. Subsequently, the received upstream wireless signal after 0.4 m air propagation are used to modulate these two CWs by two MZMs. The generated two optical signals are then coupled into the core 3 and core 4 of the MCF. After 20 km MCF propagation, the upstream signals are captured by two 10 GHz PDs and the 25 GSa/s digital sampling oscilloscope (DSO, Tektronix DPO72504DX). The same digital signal process as used in downstream transmission is performed, and the net rat of the upstream is also 4.42 Gb/s, due to the use of the same modulation parameters.

Inset (ii) and (iii) of the Fig. 3 are the received optical spectra of the optical signals before PD in the downlink and uplink respectively, and both inter-core and Rayleigh scatter crosstalk could be clearly observed. For the downstream transmission, the optical signal in core 1 and core 2 are influenced by not only the Rayleigh scatter crosstalk from the optical signal in core 3 and core 4, but also the inter-core crosstalk from the optical signal in middle core. Therefore, the sub peak at 1549.586 nm could be clearly observed in inset (ii) of the Fig. 3. However, for the upstream transmission, the optical signal in core 3 and core 4 are only influenced by the Rayleigh scatter crosstalk from the core 1, core 2, and middle core. The negligible sub peak at 1549.43 nm in the inset (iii) of Fig. 3 illustrate that the Rayleigh scatter crosstalk is obviously lower than the inter-core crosstalk in this MCF.

Fig. 4(a) shows the measured BER performance in terms of received optical power in the PD for 2×2 MIMO-OFDM/OQAM with 20 km MCF and without air transmission in both uplink and downlink. It could be clearly observed that the receiver's sensitivity at the forward-error correction (FEC) limit (BER of 3.8×10^{-3}) are -9.86 dBm and -8.83 dBm for two channels of the downlink respectively, and -10 dBm and -9.13 dBm for two channels of the uplink, respectively. The power penalty between each channel in both downlink and uplink could be attributed to the different performance of optical and electrical components. The insets in Fig. 4(a) are the received constellations of four cores when the received optical power at the PDs are -7 dBm.

Fig. 4(b) shows the measured BER performance for 2×2 MIMO-OFDM/OQAM with 20 km MCF and 0.4 m air transmission in both uplink and downlink. For downlink transmission, the receiver sensitivity for two channels at 3.8×10^{-3} FEC limit is -7.39 dBm and -6.67 dBm, respectively.

Compared to Fig. 4(a), about 2.5 dB power penalty is observed when the wireless link is added. This could be attributed to the decreased signal to noise ratio (SNR) in the air transmission. For uplink transmission, the receiver sensitivity for two channels at 3.8×10^{-3} FEC limit is -9.01 dBm and -7.56 dBm respectively. Similarly, about 1.2 dB power penalty is observed due to the decreased SNR. Different power penalty in uplink and downlink could be explained by the different position of wireless link. In downstream transmission, each MIMO signal is launched into MCF and then into air transmission link. However, in upstream transmission, each MIMO signal is launched into air link and then into MCF. Noting that the crosstalk between antennas is larger than inter-core crosstalk in MCF. As mentioned in Section 2, the different channel noise items will have different influence to the used LS MIMO equalization algorithm. Besides, the different optical and electronic components in uplink and downlink will also change the trends of BER curves. The insets in Fig. 3(b) are the received constellations at the received power of -4 dBm for both downlink and uplink, respectively.

It should be noted that only two 2×2 MIMO is investigated in our experiment due to the limitation of the channel numbers of the used AWG. However, the 2×2 MIMO channel estimation algorithm could be easily extended to N $\times$ N MIMO channel estimation algorithm when more than two input signal are transmitted. Moreover, our group has designed 64-core trench-assisted multicore fiber with maximum crosstalk less than -14 dB/20 km [21], by utilizing the heterogeneous core with the trench-assisted index profile. Therefore, we believe that the proposed scheme has potential application in future 5G cellular systems with a higher density or radio-access points.

4. Conclusion

We have experimentally demonstrated a bidirectional transmission and massive MIMO enabled radio over seven-core fiber system with centralized optical carrier delivery. In our experiment, the middle core is used to deliver the seed light to ONU for coreless upstream transmission. By using spectral efficiency OFDM/OQAM modulation technique and hybrid optical and the wireless MIMO channel estimation algorithm, bidirectional transmission of a 4.42 Gb/s 2×2 MIMO-OFDM/OQAM signal over a 20 km seven-core fiber and a 0.4 m wireless link are successfully achieved. These results show that the multicore fiber could satisfy the transparently transmission of bidirectional RF MIMO signals. Moreover, by using higher core density MCF, this architecture could be easily extended to support massive MIMO ROF transmission in future 5G cellular communication.

References

[1] J. G. Andrews *et al.*, "What will 5G be?" *IEEE J. Sel. Areas Commun.*, vol. 32, no. 6, pp. 1065–1082, Jun. 2014.
[2] S. E. Alavi, M. R. K. Soltanian, I. S. Amiri, M. Khalily, A. S. M. Supa'at, and H. Ahmad, "Towards 5G: a photonic based millimeter wave signal generation for applying in 5G access fronthaul," *Sci. Rep.*, vol. 6, no. 19891, pp. 1–11, Jan. 2016.
[3] M. Morant, J. Prat, and R. Llorente, "Radio-over-fiber optical polarization-multiplexed networks for 3GPP wireless carrier-aggregated MIMO provision," *J. Lightw. Technol.*, vol. 32, no. 20, pp. 3721–3727, Oct. 2014.
[4] T. Kanesan, S. Rajbhandari, E. Giacomidis, and I. Aldaya, "Nonlinear limit of alternative method to 2×2 MIMO for LTE RoF system," *Electron. Lett.*, vol. 50, no. 4, pp. 300–301, Feb. 2014.
[5] C. Li *et al.*, "Experimental demonstration of 429.96-Gb/s OFDM/OQAM-64QAM over 400-km SSMF transmission within a 50-GHz grid," *IEEE Photon. J.*, vol. 6, no. 4, pp. 1–8, Aug. 2014.
[6] M. Xu, J. Zhang, F. Lu, Y. Wang, D. Guidotti, and G. K. Chang, "Investigation of FBMC in mobile fronthaul networks for 5G wireless with time-frequency modulation adaptation," in *Proc. Opt. Fiber Commun. Conf. (Opt. Soc. Amer.)*, 2016, Paper W3C.2.
[7] V. Jungnickel *et al.*, "The role of small cells, coordinated multipoint, and massive MIMO in 5G," *IEEE Commun. Mag.*, vol. 52, no. 5, pp. 44–51, May 2014.
[8] L. Deng *et al.*, "2×2 MIMO-OFDM Gigabit fiber-wireless access system based on polarization division multiplexed WDM-PON," *Opt. Exp.*, vol. 20, no. 4, pp. 4369–4375, Feb. 2012.
[9] P. T. Dat, A. Kanno, N. Yamamoto, and T. Kawanishi, "WDM RoF-MMW and linearly located distributed antenna system for future high-speed railway communication," *IEEE Commun. Mag.*, vol. 53, no. 10, pp. 86–94, Oct. 2015.
[10] M. Morant, A. Macho, and R. Llorente, "On the suitability of multicore fiber for LTE-advanced MIMO optical fronthaul systems," *J. Lightw. Technol.*, vol. 34, no. 2, pp. 676–682, Jan. 2016.
[11] A. Macho, M. Morant, and R. Llorente, "Impact of inter-core crosstalk in radio-over-fiber transmission on multi-core optical media," in *Proc. SPIE OPTO (Int. Soc. Opt. Photon.)*, Feb. 2016, Art. No. 97720O.
[12] J. He *et al.*, "Experimental investigation of inter-core crosstalk tolerance of MIMO-OFDM/OQAM radio over multicore fiber system," *Opt. Exp.*, vol. 24, no. 12, pp. 13418–13428, Jun. 2016.

[13] J. M. Galve, I. Gasulla, S. Sales, and J. Capmany, "Reconfigurable radio access networks using multicore fibers," *J. Lightw. Technol.*, vol. 52, no. 1, pp. 1–7, Jan. 2016.
[14] J. Zhao, "Channel estimation in DFT-based offset-QAM OFDM systems," *Opt. Exp.*, vol. 22, no. 21, pp. 25651–25662, Oct. 2014.
[15] Y. Sasaki, Y. Amma, K. Takenaga, S. Matsuo, K. Saitoh, and M. Koshiba, "Investigation of crosstalk dependencies on bending radius of heterogeneous multicore fiber," in *Proc. Opt. Fiber Commun. Conf. (Opt. Soc. Amer.)*, Mar. 2013, Paper OTh3K.3.
[16] S. Matsuo *et al.*, "Crosstalk behavior of cores in multi-core fiber under bent condition," *IEICE Electron. Exp.*, vol. 8, no. 6, pp. 385–390, 2011.
[17] E. Kofidis, D. Katselis, A. Rontogiannis, and S. Theodoridis, "Preamble-based channel estimation in OFDM/OQAM systems: a review," *Signal Process.*, vol. 93, no. 7, pp. 2038–2054, Jul. 2013.
[18] J. He *et al.*, "2 $\times$ 2 PolMux-MIMO RoF system employing interference cancellation based OFDM/OQAM technique," in *Proc. CLEO: Sci. Innovations (Opt. Soc. Amer.)*, 2016, Paper STh1F.3.
[19] B. Li *et al.*, "Experimental demonstration of large capacity WSDM optical access network with multicore fibers and advanced modulation formats," *Opt. Exp.*, vol. 23, no. 9, pp. 10997–11006, Apr. 2015.
[20] Z. Feng *et al.*, "Multicore-fiber-enabled WSDM optical access network with centralized carrier delivery and RSOA-based adaptive modulation," *IEEE Photon. J.*, vol. 7, no. 4, pp. 1–9, Aug. 2015.
[21] B. Li, M. Tang, L. Huo, L. Deng, S. Fu, and P. P. Shum, "64 core ultra dense multicore fiber design for optical fronthaul systems," in *Proc. Specialty Opt. Fibers (Opt. Soc. Amer.)*, 2016, Paper SoM2F-2.